during this time. It follows from Eq. (2.1) that a hold of 15-20 min at fixed T_1 is sufficient. Let us study the case $t_* = 20$ min. We take the following temperature intervals: $\Delta T = 100$, 200, and 300 K. As in the experiments in [3], we take the same value for the lower temperature in all of the cycles: $T_0 = 283$ K. Then $T_1 = 383$, 483, and 583 K for all of the chosen temperature intervals. Inserting the values of T_1 and ΔT into Eq. (2.1) at $t = t_* = 1200$ sec, we obtain the corresponding growth coefficients: $\gamma_1 = 1.37 \cdot 10^{-5}$, $\gamma_2 = 7.1 \cdot 10^{-5}$, $\gamma_3 = 20 \cdot 10^{-5}$ 1/cycle.

A line is drawn through the theoretical values of the growth coefficient in Fig. 2. The experimental results are shown by points. The positions of the points shows that the results obtained theoretically agree completely with the experimental data.

LITERATURE CITED

1. É. I. Blinov and K. N. Rusinko, "Generalized theory of low-temperature deformation," Zh. Prikl. Mekh. Tekh. Fiz., No. 5 (1987).
2. N. N. Davidenkov and V. A. Likhachev, Irreducible Deformation of Metals during Cyclic Thermal Loading [in Russian], Mashgiz, Moscow (1962).
3. N. N. Davidenkov, V. A. Likhachev, and G. D. Malygin, "Study of irreversible strain caused by thermal cycling," Fiz. Met. Metalloved., 10, No. 3 (1960).

BEHAVIOR OF RUBBER IN SHOCK WAVES AND RAREFACTION WAVES

Yu. B. Kalmykov, G. I. Kanel',
I. P. Parkhomenko, A. V. Utkin,
and V. E. Fortov

UDC 532.598:678.01

There is no literature data on the properties of filled elastomers under shock-loading conditions. Despite this, rubber-like materials are used to damp pulses from shock compression and to solve other practical problems. The behavior of such materials under normal conditions is distinguished by several specific features [1, 2]; it is interesting to determine the degree to which these features of filled elastometers are manifest during intensive shock loading.

The present article reports results of the recording of the shock compression, unloading, and dynamic tension of vacuum-treated white rubber of grade 7889.

The specimens were cut from a sheet 1 cm thick. The measured density of the specimens was 1.34 g/cm^3. The speed of sound at atmospheric pressure was 1.5 km/sec. Tests in simple tension conducted at a rate of 10^{-2}-10^{-3} sec^{-1} showed that the initial Young's modulus of the rubber lies within the range 2-3 MPa, while the true breaking stress $S_n = 88$ MPa. At the moment of rupture, the relative elongation of the working part of the specimen was 609%. The permanent set after rupture was about 10%.

Plane shock waves (SW) were created in the specimens by strikers 2-7 mm thick made of aluminum or organic glass, as well as by the explosive detonation of lenses in direct contact with the specimen. The strikers were propelled by explosive devices described in [3, 4]. The pressure associated with the shock compression was varied by changing the velocity of the strikers and by using shields with different dynamic stiffnesses. The shields were placed between the striker and the specimen. We used manganin transducers to record the pressure profile P(t) in the specimen at the boundary with the shield and at a prescribed distance from it. We also used the method of Doppler laser interferometry [5, 6] to record the velocity profiles of the rear surface of the specimens u(t) in cases when the pressure pulse exited into a barrier with a low dynamic stiffness or into air.

Figure 1 shows results of measurements of the evolution of pressure profiles 1-4 in the rubber. These results are for the loading conditions shown in Table 1. No qualitative features connected with the specific properties of the rubber were seen on the P(t) profiles in the investigated range of pressures from 2 to 6 GPa. The incompleteness of the unloading

Chernogolovka. Translated from Zhurnal Prikladnoi Mekhaniki i Tekhnicheskoi Fiziki, No. 1, pp. 126-130, January-February, 1990. Original article submitted March 1, 1988; revision submitted August 19, 1988.

0021-8944/90/3101-0116$12.50

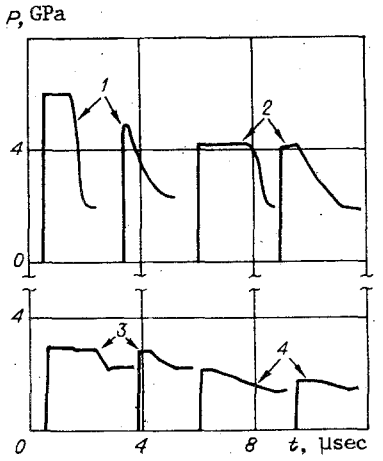

Fig. 1

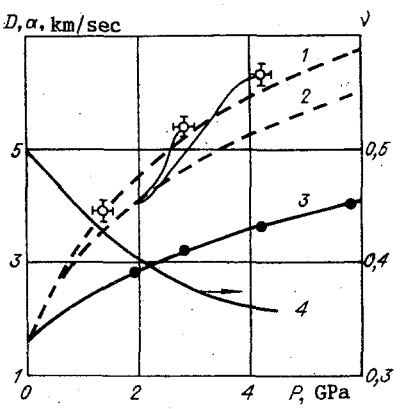

Fig. 2

TABLE 1

Profile (Fig. 1)	P, GPa	D, km/sec	u, km/sec	$\frac{V}{V_0}$	c, km/sec
1	5,80	4,02	1,10	0,726	—
2	4,20	3,65	0,88	0,760	4,80
3	2,80	3,20	0,67	0,792	4,33
4	1,95	2,84	0,52	0,816	—
4	1,36	—	—	—	3,18

in the rarefaction waves can be attributed to the relatively high dynamic stiffness of the strikers and shields used in the tests.

The measurements were used to directly determine the pressure of the shock compression P, the SW velocity D, and the Lagrangian velocities of the front and subsequent sections of the rarefaction wave $a(P) = c(P)V_0/V$. Table 1 shows the results of the measurements and the values of mass velocity u, degree of compression V/V_0, and speed of sound in the shock-compressed rubber c determined from these measurements. With allowance for the measured speed of sound at atmospheric pressure, the Hugoniot curve of the rubber in the investigated range is described by the following expression with an error equal to the measurement error

$$D = 1.5 + 2.89u - 0.53u^2, \tag{1}$$

where D and u are in km/sec.

The results of measurements of the Lagrangian velocities of the front of the rarefaction waves are shown by the clear points in Fig. 2, with an indication of the experimental error. The solid curves originating from these points correspond to the Lagrangian velocity of propagation of fixed levels of pressure in the unloading waves. Also shown are measured values of SW velocity (dark points) and the Hugoniot curve (curve 3) constructed from Eq. (1). Curve 2 is the dependence of the Lagrangian speed of sound on pressure calculated in a quasi-acoustic approximation, i.e., with the assumption that the Hugoniot curve and the isentropic unloading curve coincide in the coordinates P vs u. The quasi-acoustic approximation provides good agreement with the results of measurement of the bulk speed of sound in metals [7] within a wide range of shock pressures. The upper bound for the bulk speed of sound is the derivative $c_H = (dP/d\rho)^{1/2}$ along the Hugoniot curve; when this quantity is equal to the equilibrium speed of sound, the Grüneisen coefficient of the substance is equal to zero. Curve 1 in Fig. 2 is the relation $a_H(P) = c_H(P)V_0/V$. It is evident that the velocities of the rarefaction wavefront are roughly half as great or greater than $a_H(P)$. In other words, the front of the rarefaction wave in shock-compressed rubber propagates at a velocity in excess of the equilibrium value of the bulk speed of sound.

The high velocities of the rarefaction wave – almost twice as great as the corresponding values of shock-wave velocity – lead to rapid decay of the shock wave in the rubber. This makes it an efficient material for damping shock-wave effects.

As unloading proceeds, the measured phase velocity in the wave approaches curve 2 (Fig. 2), calculated in the quasi-acoustic approximation. It is natural to link the character of the change in phase velocities in the rarefaction wave with the elastoplastic properties of

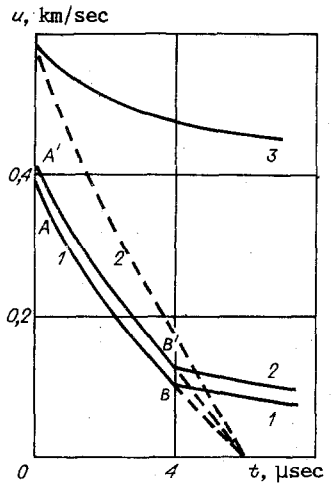

Fig. 3

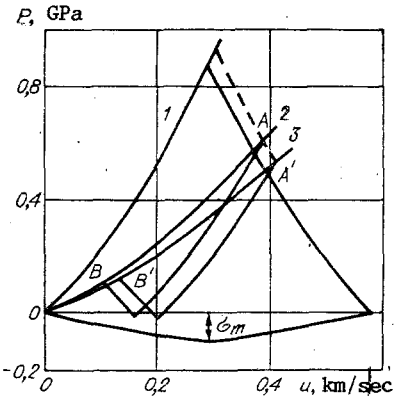

Fig. 4

shock-compressed rubber. In this case, taking curve 2 as the pressure dependence of the speed of sound, we can evaluate the Poisson's ratio of shock-compressed rubber

$$\nu = \frac{3(c_b/c_l)^2 - 1}{3(c_b/c_l)^2 + 1},$$

where c_b and c_ℓ are the bulk and longitudinal speeds of sound. The results of such an evaluation are shown in Fig. 2 (curve 2). It is evident that as shock pressure increases, the Poisson's ratio of the rubber decreases from a value close to the typical value of 0.5 for elastomers (ν_0 = 0.4998) to a value of 0.36 at a pressure of 4.2 GPa. This latter value is more typical of solids. This means that the rubber becomes glass-like under the influence of high pressure. Vitrification of rubber under the influence of pressure at room temperature was seen in [8] in tests which subjected the specimen to static pressure. Here, the Young's modulus and yield point of the material increased by two-three orders of magnitude with a narrow range of pressure.

To determine the dynamic tensile strength of rubber, we recorded velocity profiles u(t) for the rear surface of specimens in contact with a barrier made of a material with a low dynamic stiffness. The same setup was used previously to study fragmentation effects in liquids [1] and solids [10]. The measurements were conducted by Doppler laser interferometry. To reflect the probing radiation, aluminum foil 20 μm thick was stuck to the specimen surface. The pulses of shock compression were excited in specimens 10 mm thick by 2-mm-thick strikers of organic glass traveling at 850 m/sec. The Hugoniot curves of Plexiglas and rubber are close, so the use of the former as the material of the striker and shield ensures complete unloading in the first rarefaction wave.

The measurement results are shown in Fig. 3, where curve 1 was obtained in a test with a barrier consisting of ethanol. Curve 2 was obtained in a test with a barrier consisting of hexane. Information on the shock compressibility of these substances was taken from [11, 12]. With allowance for the speed of sound at atmospheric pressure, the Hugoniot curves of the barrier materials in the pressure range up to 10 GPa were represented in the form $D = 1.08 + 2.23u - 0.197u^2$ for hexane and $D = 1.16 + 2.23u - 0.181u^2$ for ethanol.

The pressure pulse at the exit of the specimen has a triangular profile and is quite attenuated. A sharp reduction in the curvature of the rarefaction wave is recorded on the u(t) profiles 4 μsec after the SW reaches the contact surface. This discontinuity is obviously the result of wave interactions in the specimen. Figure 4 shows curves depicting the change in state with interaction of the waves in the coordinates P vs u. The numbers 1-3 denote the Hugoniot curves of rubber, ethanol, and hexane, while the dashed line shows the adiabatic curves for the unloading of the rubber in tests with hexane and ethanol corresponding to a striker velocity of 850 m/sec. The numbers correspond to the notation in Fig. 3. A reflected rarefaction wave appears in the specimen after the SW reaches the interface with the barrier. The interaction of the rarefaction wave with the incident wave leads to an additional drop in pressure. As a result, tensile stresses are created in the specimen. The magnitude of these stresses is determined on the P vs u diagram by the intersection of the paths of the changes of state along the corresponding c_+ and c_- characteristics. Analysis of the P vs u diagrams shows that the points of inflection B and B' on the

u(t) profiles correspond to the attainment of zero pressure or a pressure which is somewhat lower (on the order of 10 MPa) in the specimen. This means that the appearance of the inflection points on the u(t) profile can be attributed to rupture of the rubber under the influence of small tensile stresses. The subsequent slow decrease in velocity is then explained by re-reflection of the rarefaction wave from the rupture surface. However, the proposition that rubber has a low tensile strength is inconsistent with the results of static tests.

If the strength of a body is negligibly low, then the velocity of a shock wave should remain constant after it reaches the free surface of the body, regardless of the reduction in parameters in the loading pulse. Figure 3 shows the velocity profile of the surface of the rubber specimen when the SW exits into air (curve 3). The velocity of the Plexiglas striker in this test was roughly 5% lower than in the preceding experiments. The dashed line in Fig. 3 shows the velocity profile of the free surface of the specimen calculated from the results of tests conducted with barriers when it was presumed that the specimen remained intact.

The measured velocity profile of the free surface differs from the profiles for the extreme cases of high and negligibly low dynamic tensile strength for rubber. The central part of the specimen remained intact through the entire thickness in this test. Visual inspection of the axial section of the specimen with the naked eye and with a microscope having a magnification up to ×100 failed to show signs of rupture. Thus, the behavior of rubber under dynamic tension is characterized by significant differences from the cases of solids or liquids.

It is known [13] that the rupture of an elastometer is preceded by the formation of microscopic discontinuities in the specimen. These discontinuities begin to form at stresses much lower than the breaking stresses. The formation of the discontinuities in and of itself – due to delamination or pore formation – does not constitute rupture. Thus, in tests in which vulcanized rubber was subjected to triaxial tension [14], cavities began to form at stresses of 1-3 MPa and a low strain level; the specimens then underwent further deformations of several hundred percent and a simultaneous increase (with a low absolute value) in the tensile stresses. The deformation regime in the neighborhood of the cavities deviated from triaxiality after the cavities were formed, and the formation of large reversible strains became possible.

These features of the deformation of elastomers explain the anomalous behavior of the rubber in dynamic tension. The formation and reversible growth of cavities lead to a reduction in the bulk modulus of elasticity and the speed of sound in the rubber in the region of negative pressures. The decrease in sonic velocity in turn causes a reduction in the curvature of the rarefaction wave on the velocity profile on the specimen's free surface.

The Lagrangian speed of sound a_t in tensioned rubber can be evaluated by comparing the actual and theoretical (with the assumption of retention of the initial bulk modulus of elasticity) curvatures of the velocity profile of the free surface. If we assume that zero pressure is reached on a certain curve having the slope c_0 in the coordinates distance x vs time t during the interaction of the incident and reflected waves and that the sudden change in the elastic modulus occurs when the pressure is equal to zero, then from a simple analysis of t vs x curves of the process we obtain $a_t^+ = c_0/(2\dot{u}_t^+/\dot{u} - 1)$, where $\dot{u}_t^+$, $\dot{u}$ are the curvatures of the theoretical and experimental velocity profiles of the free surface. In the case being examined, u_t = 100 m/(sec·μsec) u = 30 m/(sec·μsec). Taking c_0 equal to the speed of sound under normal condition (c_0 = 1.5 km/sec), we find a_t = 0.27 km/sec for the initial section of the experimental u(t) profile. It can be seen from Fig. 3 that the curvature of the measured u(t) profile still decreases over time, which is evidence of a further reduction in the bulk modulus of elasticity.

Knowing the speed of sound, we can evaluate the slope $dP/du = \pm\rho_0 a$ of the path of change of the state of the rubber along the characteristic for the region $P < 0$. Thus, we can also evaluate the maximum tensile stresses which occur in the experiments in which the rubber was unloaded in air. The corresponding curves are shown in Fig. 4. It follows from this figure that the decrease in velocity seen in Fig. 3 (curve 2) corresponds to the attainment of a tensile stress no greater than 20 MPa. The highest negative stresses σ_m that can be reached in rubber under the given loading conditions are estimated to be 100 MPa.

Thus, the results of our experiments illustrate specific features of the behavior of rubber under shock loading. The differences in the dynamic properties of rubber are related

to its hardening under the influence of shock compression and the potential for the reversible growth of discontinuities during dynamic tension.

We thank V. É. Zgaevskii and V. K. Golubev for their discussion of the findings.

LITERATURE CITED

1. M. P. Bukhina, Theoretical Physics of Elastomers [in Russian], Khimiya, Moscow (1984).
2. A. A. Askadskii, Deformation of Polymers [in Russian], Khimiya, Moscow (1973).
3. G. I. Kapel', A. M. Molodets, and A. A. Vorob'ev, "Projection of plates by an explosion," Fiz. Goreniya Vzryva, No. 6 (1974).
4. G. I. Kanel', "Resistance of metals to cleavage fracture," Fiz. Goreniya Vzryva, No. 3 (1982).
5. J. R. Asay and L. M. Barker, "Interferometric measurement of shock-induced internal particle velocity and spatial variations of particle velocity," J. Appl. Phys., 45, No. 6 (1974).
6. M. I. Belovolov, V. I. Vovchenko, et al., "Use of laser-interferometric velocity meters in explosion experiments," Zh. Tekh. Fiz., 57, No. 5 (1987).
7. A. N. Dremin and G. I. Kanel', "Refraction of the front of an oblique shock wave at a boundary with a less stiff medium," Zh. Prikl. Mekh. Tekh. Fiz., No. 3 (1970).
8. C. W. Weaver and M. S. Paterson, "Stress–strain properties of rubber at pressures above the glass transition temperature," J. Polym. Sci., 7, Pt. A-2, No. 3 (1969).
9. D. C. Erlich, D. C. Wooten, and R. C. Crewdson, "Dynamic tensile failure of glycerol," J. Appl. Phys., 42, No. 13 (1971).
10. G. W. Stepanov, Behavior of Structural Materials in Elastoplastic Loading Waves [in Russian], Naukova Dumka, Kiev (1978).
11. J. M. Walsh and M. H. Rice, "Dynamics of liquids from measurements on strong shock waves," J. Chem. Phys., 26, No. 4 (1957).
12. I. J. Ahrens and M. H. Ruderman, "Immersed-foil method for measuring shock wave profiles in solids," J. Appl. Phys., 37, No. 13 (1966).
13. F. R. Eirich and T. L. Smith, "Molecular-mechanical aspects of the isothermal rupture of elastomers," in: Fracture [Russian translation], Vol. 7, Part 2, Mir, Moscow (1976).
14. A. N. Gent and P. B. Lindley, "Internal rupture of bonded rubber cylinders in tension," Proc. R. Soc. London, 249, Ser. A, No. 1 (1959).

MOVEMENT OF THE FREE BOUNDARY OF A HALF-SPACE DURING THE PROPAGATION OF AN OBLIQUE STRAIGHT CRACK

V. A. Saraikin

UDC 539.375

Internal defects which grow dynamically in a material generate disturbances. The elastic model of the propagation of a dislocational discontinuity [1-4] is widely used in geophysics to identify the type, orientation, and size of large-scale defects – earthquake foci [1-4]. In accordance with this model, a jump in the displacement vector is assigned at the site of the discontinuity to describe the advance of the edges of the latter. This description is independent of the details of the distribution of the initial internal stress field. The orientation of the nodal planes found by this approach agrees poorly with experimental findings when the discontinuity is of the shear type. When an appropriate choice is made for the jumps in the displacements, the asymptote of the solution in the long-range field for a dislocational discontinuity differs little from the solution of the problem for a point source given by force couples without moments.

A method of describing a discontinuity (crack) which is exact within the framework of linear fracture mechanics involves specifying a drop in stress on the discontinuity [2]. The displacement field and the orientation and size of the crack in this model are consistent with the stress field, which itself conforms to the condition of dynamic instability at the crack tip.

Novosibirsk. Translated from Zhurnal Prikladnoi Mekhaniki i Tekhnicheskoi Fiziki, No. 1, pp. 130-136, January-February, 1990. Original article submitted August 24, 1988.

 0021-8944/90/3101-0120$12.50